Rheology of hyperbranched polymer melts undergoing planar Couette flow

T. C. Le,[1] B. D. Todd,[1,a)] P. J. Daivis,[2] and A. Uhlherr[3]
[1]*Centre for Molecular Simulation, Swinburne University of Technology, P.O. Box 218, Hawthorn, Victoria 3122, Australia*
[2]*School of Applied Sciences, RMIT University, GPO Box 2476V, Melbourne 3001, Victoria, Australia*
[3]*CSIRO Information Management and Technology, Private Bag 33, Clayton South, Victoria 3169, Australia*

(Received 1 April 2009; accepted 2 July 2009; published online 23 July 2009)

The melt rheology of four hyperbranched polymer structures with different molecular weights has been studied using nonequilibrium molecular dynamics (NEMD). Systems were simulated over a wide range of strain rates to capture the crossover behavior from Newtonian to non-Newtonian regimes. Rheological properties including shear viscosity and first and second normal stress coefficients were computed and the transition to shear thinning was observed at different strain rates for hyperbranched polymers of different sizes. The results were consistent with previous findings from NEMD simulation of linear and dendritic polymers. Flow birefringence was characterized by taking into account both form and intrinsic birefringences, which result from molecular and bond alignment, respectively. The stress optical rule was tested and shown to be valid only in the Newtonian regime and violated in the strong flow regime where the rule does not take into account flow-induced changes of the microstructure. © *2009 American Institute of Physics*.
[DOI: 10.1063/1.3184799]

I. INTRODUCTION

Dendritic polymers including dendrimers and hyperbranched polymers are a class of highly branched polymers that have unique properties due to their molecular architectures.[1] Dendrimers with perfectly branched structures are more difficult to synthesize due to the requirement of chemical purity and stringent multiprocessing steps. In contrast, hyperbranched polymers with imperfect branching can be prepared easily using "one-pot" techniques that save time and are suitable for large scale, low cost production. However the one-pot techniques provide a polydisperse mixture of randomly branched polymers with different size and topology. This leads to difficulties in experiments but it gives simulation a valuable opportunity to shed light on the structure and rheology of monodisperse melts of hyperbranched polymers. In our previous report,[2] the structural properties of four hyperbranched polymer topologies under shear flow were analyzed. In this subsequent paper, the rheological properties of those fluids will be discussed.

Possessing special structures, dendritic polymers including dendrimers and hyperbranched polymers have many interesting properties. One of the most interesting physical properties is the unusual melt rheology, which suggests that these macromolecules have potential application as rheology modifiers and processing aids.[3] In comparison with linear polymers, dendrimers and hyperbranched polymers possess much lower viscosity and very high solubilities due to their packed structure with a large number of functional end groups in one molecule. It has been demonstrated that dendritic polyether and poly(amidoamine) melts exhibit a Newtonian behavior over the available measurement range in experiments and the lack of entanglements in the systems observed suggests that as the dendritic topology leads to globular conformations, molecules do not interpenetrate significantly in the melt and do not combine to form aggregated structures.[4] In the case of dendritic polymers in solution, a peak is observed in the plot of intrinsic viscosity versus molecular mass.[5] This is in contrast with linear chains which obey the Mark–Houwink equation[6] and show a steady increase in the intrinsic viscosity as a function of molecular weight.

Although the number of experimental papers on hyperbranched polymers has increased considerably, only a few of them focus on rheology and especially melt rheology of these materials. One of the earliest studies on melt rheology of hyperbranched polymers was reported by Farrington *et al.*[7] in 1998. The melt viscosities of dendritic poly(benzyl ether) including dendrimers and some end-substituted mono- and tridendrons were measured. Hsieh *et al.*[8] then presented rheological properties of processed commercial aliphatic hyperbranched polyester melts. Shear thinning was observed for the lower generation, whereas Newtonian behavior was exhibited by the higher generation hyperbranched polyesters. It was also found that blends of these commercial polyesters showed only Newtonian behavior under both steady shear and oscillatory shear if at least one of them is Newtonian. Another early study on melt rheology reported by Kharchenko *et al.*[9] characterized the behavior of hyperbranched polystyrenes. This was also the first publication on flow birefringence of this polymer. It was found that hyperbranched polystyrenes showed nonterminal behavior in the low-frequency rheological response and the stress optical rule (SOR) was only valid for polymers of high molecular weights. Moreover it was shown that when this rule holds, the stress optical coefficient for hyperbranched polystyrenes

a)Electronic mail: btodd@swin.edu.au.

was much lower than that for linear analogs. After that, Suneel *et al.*[10] reported their studies on melt rheology and molecular weight distribution of short chain hyperbranched aromatic polyesters. These papers confirmed that in hyperbranched polymer melts the chains are essentially unentangled. Another study on hyperbranched polyesters reported by Gretton-Watson *et al.*[11] showed that the viscosity of hyperbranched poly(methylmethacrylate) melt was significantly lower than that of linear chains and exhibited shear thinning behavior.

As presented in our previous paper,[2] a few molecular simulation studies on hyperbranched polymer simulation have been reported. However none of them focused on melt rheology. Therefore the purpose of this paper is to report the first study on the melt rheology of hyperbranched polymers using a coarse-grained model and nonequilibrium molecular dynamics (NEMD) simulations.

A simple specific architecture of hyperbranched polymers has been studied. The hyperbranched polymers generated have the same molecular weight (number of beads) as perfect trifunctional dendrimers but fewer branches at one branching point and extra beads added in the outermost layer of the molecules. Beads along the chain interact via Weeks–Chandler–Anderson[12] (WCA) and finitely extensible nonlinear elastic[13] (FENE) potentials. More details of the hyperbranched polymer topologies and bead spring model can be found in our previous report.[2]

In the remainder of this paper, all quantities are expressed in terms of site reduced units in which the reduction parameters are the Lennard-Jones interaction parameters ε and σ and the mass $m_{i\alpha}$ of bead α in molecule i, which are set to the value of one. In terms of the corresponding quantities in real units, the reduced temperature is given by $T^*=k_BT/\varepsilon$, the density by $\rho^*=\rho\sigma^3$, the pressure tensor by $\mathbf{P}^*=\mathbf{P}\sigma^3/\varepsilon$ and strain rate by $\dot{\gamma}^*=(m_{i\alpha}\sigma^2/\varepsilon)^{1/2}\dot{\gamma}$. For simplicity of notation, the asterisk will be omitted hereafter.

To simulate fluids under shear, the molecular version of the SLLOD algorithm[14] was applied and the equations of motion are given as

$$\dot{\mathbf{r}}_{i\alpha}=\frac{\mathbf{p}_{i\alpha}}{m_{i\alpha}}+\mathbf{r}_i\cdot\nabla\mathbf{u}, \tag{1}$$

$$\dot{\mathbf{p}}_{i\alpha}=\mathbf{F}_{i\alpha}-(m_{i\alpha}/M_i)\mathbf{p}_i\cdot\nabla\mathbf{u}-\zeta(m_{i\alpha}/M_i)\mathbf{p}_i, \tag{2}$$

where $\mathbf{r}_{i\alpha}$ and $\mathbf{p}_{i\alpha}$ represent the position and thermal momentum of an bead α in molecule i, $\nabla\mathbf{u}$ is the strain rate tensor, $\mathbf{r}_i=\Sigma_{\alpha=1}^{N_\alpha}m_{i\alpha}\mathbf{r}_{i\alpha}/M_i$ is the position of the molecular center of mass of molecule i, $M_i=\Sigma_{\alpha=1}^{N_\alpha}m_{i\alpha}$ is the mass of molecule i, $\mathbf{p}_i=\Sigma_{\alpha=1}^{N_\alpha}\mathbf{p}_{i\alpha}$ is the momentum of the molecular center of mass of molecule i, and ζ is the thermostat constraint multiplier which is given by

$$\zeta=\frac{\Sigma_{i=1}^{N}\mathbf{F}_i\cdot\mathbf{p}_i-\dot{\gamma}\Sigma_{i=1}^{N}p_{ix}p_{iy}}{\Sigma_{i=1}^{N}\mathbf{p}_i^2}. \tag{3}$$

This expression for ζ is derived from Gauss' principle of least constraint and used to keep the molecular center of mass kinetic temperature constant. Throughout the simulation, there was only one single thermodynamic state point defined by the reduced bead density of 0.84 and the reduced temperature of 1.25. The equations of motion of atoms were integrated with time step $\Delta t=0.001$ in reduced units using a fifth-order Gear[15] predictor corrector differential equation solver. For hyperbranched polymers comprising 19 beads, *NVT* simulations were performed with 216 molecules, whereas for polymers comprising 43, 91, and 187 beads, *NVT* simulations were run with 125 molecules. Each simulation began with an equilibration period and 40 separate runs, which consist of 1×10^6 time steps each performed for every system. The mean simulation data were evaluated from results of all the separate runs.

In Sec. II A of this paper, detailed analysis and discussion of rheological properties for four different hyperbranched polymers with molecular weight lying between 19 and 187 are presented. Section II B focuses on the flow birefringence effect for hyperbranched polymers, which results from contributions from the form and intrinsic birefringence. In part C of Sec. II, comparisons with predictions of the SOR are shown. Finally, Sec. III presents a summary and conclusions.

II. RESULTS AND DISCUSSION

A. Rheology

The rheological properties of hyperbranched polymer fluids under shear flow, such as the shear viscosity and first and second normal stress coefficients, can be calculated from the components of the molecular pressure tensor[16] given by

$$\mathbf{P}^MV=\left\langle\sum_{i=1}^{N_m}\frac{\mathbf{p}_i\mathbf{p}_i}{M_i}-\frac{1}{2}\sum_{i=1}^{N_m}\sum_{\alpha=1}^{n}\sum_{j\neq i}^{N_m}\sum_{\beta=1}^{n}\mathbf{r}_{ij}\mathbf{F}_{i\alpha j\beta}\right\rangle, \tag{4}$$

where $\mathbf{p}_i$ represents the total peculiar center of mass momentum of molecule i, as defined by the equations of motion, $\mathbf{r}_{ij}=\mathbf{r}_j-\mathbf{r}_i$ is the center of mass separation of molecule i and j, $\mathbf{F}_{i\alpha j\beta}$ is the intermolecular force on bead α in molecule i due to bead β in molecule j and n is the total number of interacting beads in a molecule. The angular brackets denote an average over the nonequilibrium steady state. The non-Newtonian shear viscosity of hyperbranched polymer fluids subject to planar shear flow, where the fluid flows in the x direction with velocity gradient in the y direction, can be calculated from the components P_{xy} and P_{yx} of the molecular pressure tensor $\mathbf{P}^M$ as $\eta=-\langle P_{xy}+P_{yx}\rangle/2\dot{\gamma}$.

The viscosities at various shear rates computed for different hyperbranched polymers using NEMD simulation are presented in Fig. 1. As can be seen, at the same strain rate, larger hyperbranched polymers have higher viscosity values, indicating that under shear they have longer relaxation times. It can also be seen that the range of strain rates considered is large enough to capture the shear thinning behavior of all simulated hyperbranched polymer systems. At low strain rates, the viscosities remain constant whereas at high strain rates, these values decrease rapidly. This property of polymeric fluids is very important for many engineering applications. Shear viscosity data for different hyperbranched polymers in Fig. 1 were fitted using the Carreau–Yasuda model[6] which is given by $\eta=\eta_0/[1+(\lambda\dot{\gamma})^2]^p$, where η_0 is the zero

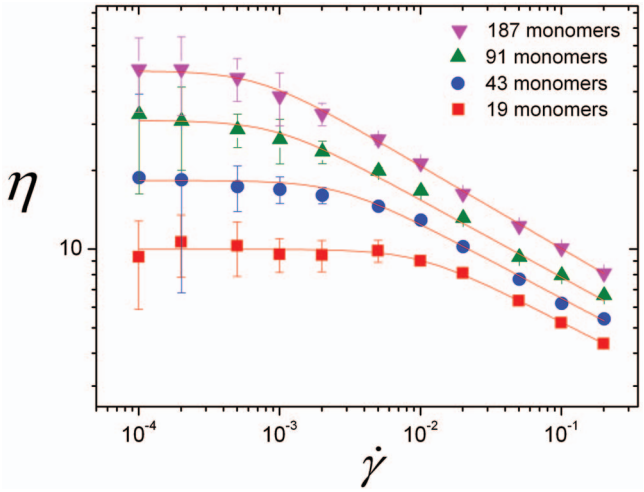

FIG. 1. Dependence of shear viscosity on strain rate for hyperbranched polymers of different molecular weights (solid lines representing fitting with the Carreau–Yasuda model).

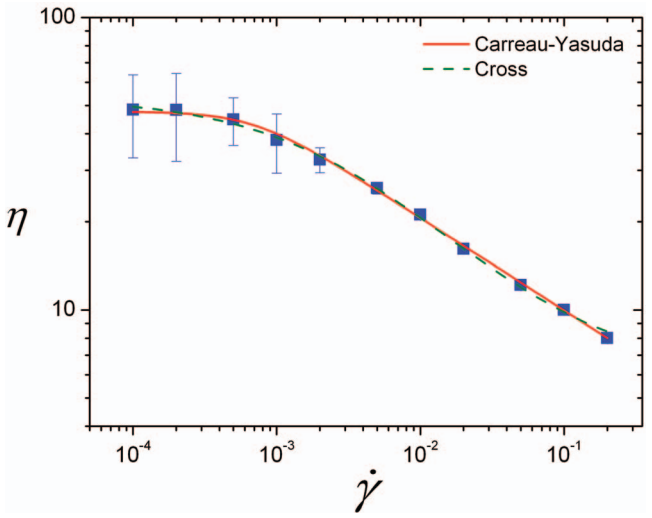

FIG. 2. Carreau–Yasuda equation vs Cross equation fitted for shear viscosity data for hyperbranched polymers composed of 187 monomers.

shear viscosity, λ is a time constant and p is the power law exponent. Table I presents the fitting parameters obtained for all simulated hyperbranched polymer systems. Apart from using the Carreau–Yasuda model, an alternative way to obtain the zero shear rate viscosity is by using the Cross equation,[17] given as $\eta=\eta_\infty+(\eta_0-\eta_\infty)/(1+(K\dot{\gamma})^m)$, where η_∞ is the infinite shear viscosity, K is the consistency index, and m is the power law index. The disadvantage of the Cross model is that in experiment, it is difficult to measure the infinite shear rate viscosity η_∞, therefore it is often set to be a very small value.[18] Figure 2 presents the fitted lines obtained from the Cross equation in comparison with the Carreau–Yasuda equation for shear viscosity data of hyperbranched polymers comprising 187 monomers. It can be seen that these two models agree very well. Fitted lines are slightly different at very high shear rates, in the transition region from Newtonian to non-Newtonian and at very low shear rates. Cross equation fitting parameters for shear viscosity data are shown in Table II. The zero shear viscosities for hyperbranched polymers composed of 19, 43, and 91 beads obtained from Cross equation fitting are quite similar to those from the Carreau–Yasuda model.

Figure 3 presents the dependence of the zero shear rate viscosity on the number of beads per molecule for different hyperbranched polymers. The zero shear rate viscosity scales as $\eta_0 \propto N^{0.657(2)}$ where N is the number of monomers/beads per molecule, where by 0.657(2) we mean 0.657 ± 0.002. The exponent of the power law for hyperbranched polymer melts is consistent with that for dendrimers which were found to have $\eta_0 \propto N^{0.646(2)}$ (Ref. 19) due to similar molecular structures. Furthermore, our results suggest that hyperbranched polymers are free of entanglements as the dependence of viscosities on the number of monomers does not break into two regions at low and high number of monomers while most of the linear analogs have viscosity dependencies given as $\eta_0 \propto M_w$ at low molecular weights and $\eta_0 \propto N^{3.4}$ at high molecular weights where the polymer chains entangle.[20] However as WCA and FENE potentials were employed to simulate hyperbranched polymers, beads along the polymer chain can vibrate and rotate freely. This results in a polymer model that is more flexible than typical real materials and model molecules in shearing dense fluids may fold upon themselves more than in reality. It has been found experimentally that the value of the power law exponent for dendrimers is ~1.1 (Refs. 7 and 21) which is quite high compared to that from NEMD simulations, which was found to be 0.646(2). Therefore higher shear viscosity and higher values of the power law exponent are expected in experiments on common hyperbranched polymers. However the comparison between our model and real polymers should be made in terms of the number of Kuhn steps per molecule, defined as $N_K=(N_s-1)^2/C_\infty$, where N_S is the number of beads and C_∞ is the characteristic ratio. The value of N_K makes it possible to estimate the molar mass of the real polymer with an equivalent N_K to the polymer simulated. Our model and a closely related model with constrained bond lengths[22] have the characteristic ratio of ~1.5–1.8, which can be compared with polyethylene which has a characteristic ratio of about 7.2.

The time constant λ in the Carreau–Yasuda model fitted

TABLE I. Parameters of the Carreau–Yasuda model fitted to the shear viscosity vs strain rate dependence.

Number of beads	η_0	λ	p
19	10(2)	101(8)	0.138(1)
43	18(3)	378(237)	0.143(5)
91	31(11)	1069(299)	0.148(8)
187	48(6)	1422(615)	0.158(2)

TABLE II. Parameters of the Cross equation fitted to the shear viscosity vs strain rate dependence.

Number of beads	η_0	η_∞	K	m
19	10(2)	4(1)	24(9)	1.3(4)
43	18.6(3)	3.2(9)	60(10)	0.78(9)
91	35(1)	2(1)	178(20)	0.56(5)
187	53(2)	6(1)	310(41)	0.71(8)

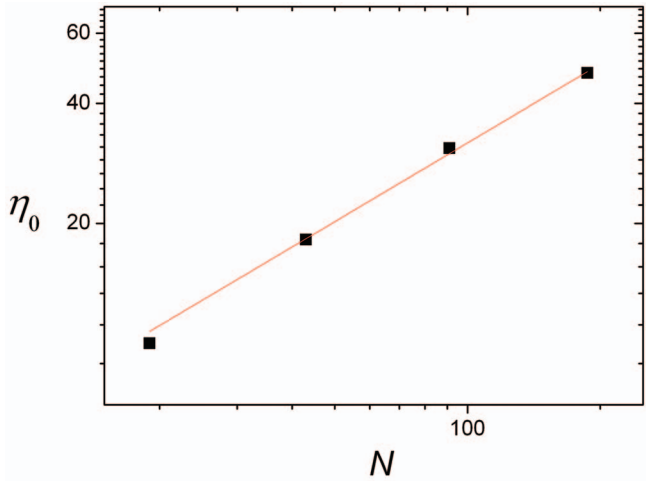

FIG. 3. Zero shear viscosity vs number of beads per molecule for hyperbranched polymers.

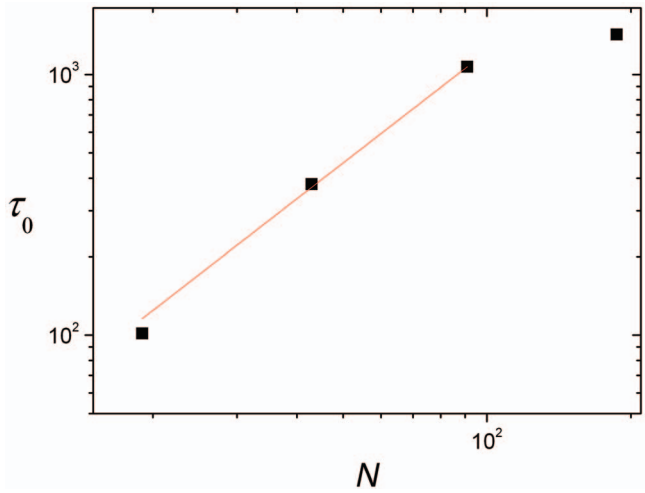

FIG. 4. Longest relaxation time vs number of beads per molecule for hyperbranched polymers.

to the simulation data is also the longest relaxation time of molecules composing the fluids. Although the longest relaxation time τ_0 can be the rotational relaxation time or the reptation relaxation time, τ_0 can be considered to be the rotational relaxation time as there is no entanglement in these hyperbranched polymer systems and hence there is no reptation relaxation time. On the other hand, the inverse of the time constant λ is the strain rate $\dot{\gamma}_0$ at which the onset of shear thinning is observed. For hyperbranched polymers with 19, 43, 91, and 187 beads, the values of $\dot{\gamma}_0$ are $9.9(5)\times10^{-3}$, $2.6(4)\times10^{-3}$, $9.35(3)\times10^{-4}$, and $7.032(2)\times10^{-4}$, respectively. The shear thinning behavior occurs at lower strain rates for large hyperbranched molecules in comparison with small hyperbranched polymers. This can be explained by relaxation times, the deformation and tendencies to align with the shear flow. Shear thinning occurs due to the deformation and increased alignment of the molecules to the flow field, which is directly related to the relaxation time τ_0.[23] At shear rates higher than the inverse of τ_0, molecules are stressed and in order to reduce the stress, the molecules extend, the deformation occurs and the alignment increases, the fluid moves into the non-Newtonian regime and the new structural configuration results in lower viscosity. Because larger molecules have longer relaxation time τ_0, the value of $1/\tau_0$ is smaller than that of small molecules and the fluids composed of large polymers exhibit the crossover from Newtonian to non-Newtonian behavior at lower strain rates. The stretching caused by the applied shear results in a more ellipsoidal configuration of hyperbranched polymers which has been discussed in detail in our previous paper.[2]

Figure 4 presents the dependence of longest relaxation time τ_0 on the number of beads per molecule N for four hyperbranched polymer systems. The logarithm of τ_0 for hyperbranched polymers composed of 19, 43, and 91 beads has a linear relationship with the logarithm of the number of beads N. The relaxation time for these systems scales as $\tau_0 \propto N^{1.4(2)}$. The exponent value of 1.4(2) for hyperbranched polymers is consistent with previous NEMD simulation results which found that the exponent value is 1.7 for linear polymers and 1.3 for dendrimers.[24] Our exponent result is lower than those predicted by the Rouse model which gives $\tau_0 \propto M^2$.[25] On the other hand the value of τ_0 for the largest hyperbranched polymer system comprising 187 beads does not follow the same trend of the smaller polymers. The main causes might be the increase in structural rigidity with the number of beads N and the flow-induced stretching behavior of hyperbranched polymers which results in the more aspherical shape of small molecules and more spherical shape of large molecules. This is opposite to the behavior of linear molecules. For long linear polymers above N_{critical}, the longest relaxation time, which is predicted to scale as N^3 by the reptation theory, results from the entanglement of long chains.[26] This is less likely to be the case for hyperbranched polymers with short branches and a large number of terminal groups. Furthermore our computed values of the longest relaxation time have large uncertainties due to the multistep procedure used to obtain them.

The Weissenberg number W_e, which is a dimensionless shear rate, can be calculated from the longest relaxation time by the definition $W_e = \dot{\gamma}\tau_0$.[6] Unlike the Deborah number which is used to describe flows with a nonconstant stretch history, the Weissenberg number describes the flow with a constant stretch history. Figure 5 presents the dependence of the ratio of shear viscosity and zero shear rate viscosity on the Weissenberg number for different hyperbranched polymers. It can be seen that the ratios of shear viscosity to zero shear rate viscosity obtained from NEMD simulations for four hyperbranched polymer systems show a significant degree of consistency with a single master curve. At $W_e \approx 1$, the value of η/η_0 for all polymers starts to decrease and the fluids move from the Newtonian to non-Newtonian regime. The computed data were fitted with the Carreau–Yasuda model and give a dependence of η/η_0 to the Weissenberg number as $\eta/\eta_0 = 0.996(9)/[1+(1.1(1)\times W_e)^2)]^{0.143(6)}$. Using the master curve established, the shear rate dependence of the viscosity of other hyperbranched polymers in this series could be predicted.

The first and second normal stress coefficients, which can be defined as $\psi_1 = \langle P_{yy} - P_{xx}\rangle/\dot{\gamma}^2$ and $\psi_2 = \langle P_{zz} - P_{yy}\rangle/\dot{\gamma}^2$, are presented in Fig. 6. These values describe the effect of

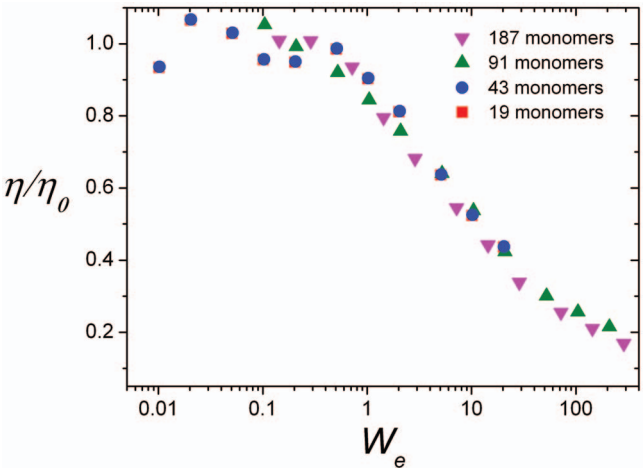

FIG. 5. Dependence of the ratio η/η_0 on the Weissenberg number for different hyperbranched polymers.

the normal stress differences exhibited by polymeric fluids. Unlike Newtonian fluids which have the normal stress differences exactly zero in shearing flow, polymeric fluids always have positive first normal stress coefficient which is usually much larger than the magnitude of the negative second normal stress coefficient.[6] An increase in these stress coefficients reflects a tendency of the fluid to deform in the normal directions under shear. For all hyperbranched polymer systems studied, the normal stress coefficients have a large power-law region in which it might decrease by as much as a factor of 10^6 for a large molecular system. Furthermore, the rate of decline of the first and second normal stress coefficients with the strain rate is much greater than that of the shear viscosity. In the low shear rate region, the normal stress coefficients reach a plateau as the ratios of $P_{yy}-P_{xx}$ and $P_{zz}-P_{yy}$ are proportional to $\dot{\gamma}^2$, whereas at higher shear rates, the values of the normal stress coefficients rapidly decrease. This again indicates that the hyperbranched polymer fluid has a crossover from Newtonian to non-Newtonian behavior. At the same strain rate, larger hyperbranched polymers have higher first and second normal stress coefficients as they tend to deform more in comparison with the small molecules. The second normal stress coefficient, which has been studied less extensively in experiments than the first coefficient, is negative and much smaller in magnitude than the first normal stress coefficient. In comparison with other simulation results,[19] our normal stress coefficient values for hyperbranched polymers are larger than those for dendrimers but smaller than those for linear polymers.

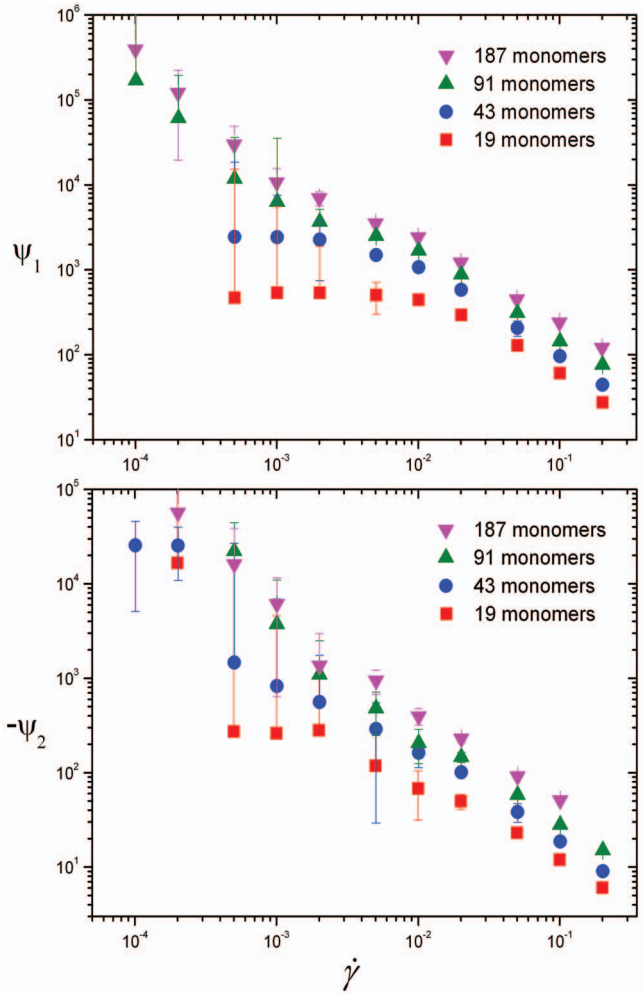

FIG. 6. First and second normal stress coefficients vs strain rate for different hyperbranched polymers.

TABLE III. Estimated values of the exponents in the power-law regions for the first and second normal stress coefficients.

Number of beads	α	β
19	1.09(4)	0.96(2)
43	1.09(2)	1.0476(9)
91	1.05(3)	0.96(2)
187	1.00(2)	0.91(3)

Data for the first normal stress coefficient for hyperbranched polymers consisting of 19 and 43 beads were fitted using the Carreau–Yasuda model. The zero shear rate first normal stress coefficients $\psi_{1,0}$ for these systems were found to be 508(13) and 2430(45), respectively. From these values and zero shear rate viscosities η_0 obtained from the Carreau–Yasuda fit for shear viscosity, the viscous relaxation time τ_v can be computed. The viscous relaxation time, which is defined by $\tau_v=\int_0^\infty tG(t)dt/\int_0^\infty G(t)dt$, where $G(t)$ is the stress relaxation modulus from the theory of linear viscoelasticity,[27] can be calculated by the expression $\tau_v=\psi_{1,0}/2\eta_0$. For hyperbranched polymers comprising 19 and 43 beads, the values of τ_v were found to be 25(3) and 67(7), respectively. These values are in very good agreement with the time constants K obtained from the Cross model which were found to be 24(9) and 60(10) for those hyperbranched polymer systems.

The normal stress coefficients for all hyperbranched polymers were fitted in the power-law region and the values of the exponents of the asymptotic dependences $\psi_1 \propto \dot{\gamma}^{-\alpha}$ and $|\psi_2| \propto \dot{\gamma}^{-\beta}$ are presented in Table III. The values of these exponents are within the range of experimental values for polymer melts and concentrated solutions.[6] Similar to NEMD simulation results for dendrimer melts,[24] the values of the α and β exponents do not vary systematically with the size of the hyperbranched polymer molecules. This is in contrast with results for linear polymers[24] which have the values of α and β increasing with the chain lengths.

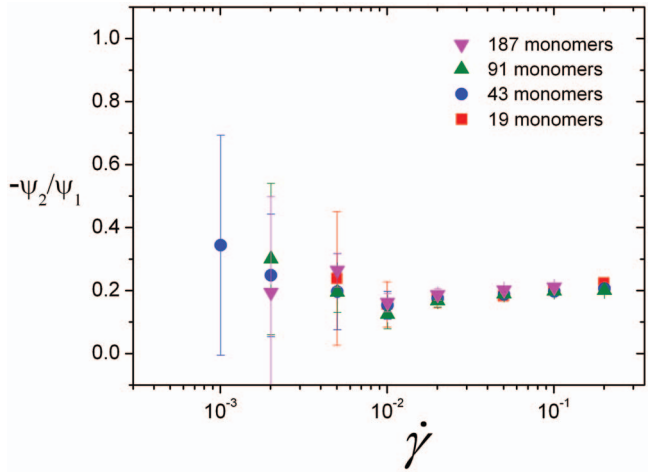

FIG. 7. Ratio of the second and first normal stress coefficients for different hyperbranched polymer systems.

The ratios of $-\psi_2/\psi_1$ are presented in Fig. 7, which shows that the values of $-\psi_2/\psi_1$ are ~0.2 for all hyperbranched polymer systems. This is very similar to simulation results for dendrimers as they all have compact, highly branched architectures with globular shape and internal bond constraints which prevent pronounced stretching of the molecules.

Figure 8 shows the isotropic pressure of the hyperbranched polymer systems under shear which was calculated as

$$p = \tfrac{1}{3}\mathrm{Tr}(\mathbf{P}^M) = \tfrac{1}{3}(P_{xx} + P_{yy} + P_{zz}). \quad (5)$$

At low strain rates, the pressure of smaller hyperbranched polymer fluids is higher than that of larger polymer fluids, while at high strain rates, the pressure of the large molecule fluids increases earlier and more rapidly than that of the small ones. This can be explained by the behavior of different molecules under shear as presented in our previous paper,[2] that larger molecules of hyperbranched polymers become aspherical more quickly under shear than for small

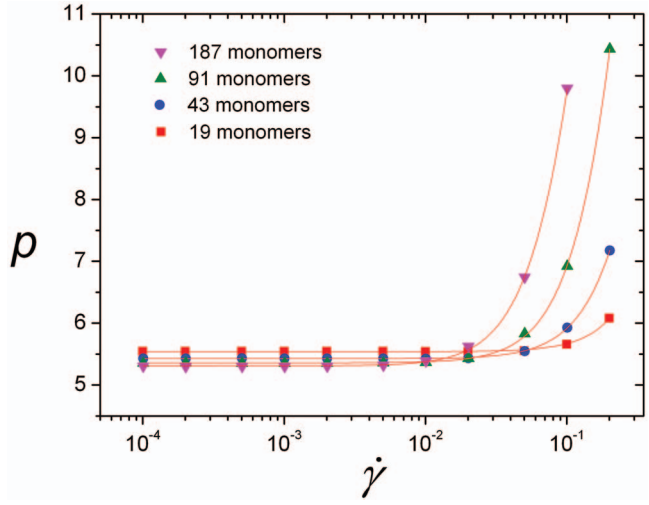

FIG. 8. Dependence of the isotropic pressure on strain rate for different hyperbranched polymers (solid lines representing fitting with the Carreau–Yasuda model).

molecules. Fitting the pressure data using the Carreau–Yasuda model $p=p_0/[1+(\lambda_p\dot{\gamma})^2]^m$ which has been applied for shear viscosity data, the zero shear pressure of hyperbranched polymers can be investigated. The values of the zero shear pressure p_0 are 5.540(3), 5.414(3), 5.349(6), and 5.299(8) for hyperbranched polymers composed of 19, 43, 91, and 187 monomers, respectively. The critical strain rate at which the transition from Newtonian to non-Newtonian behavior of the pressure occurs can be evaluated as the inverse of λ_p obtained from the Carreau–Yasuda model. The critical strain rate was found to have the value of 0.217(2), 0.126(5), and 0.06(2) for hyperbranched polymers comprising 43, 91, and 187 monomers, respectively. For hyperbranched molecules composed of 19 monomers, the value of λ_p obtained is very small and the value of the standard error is large, hence the critical strain rate calculated is uncertain. In comparison to the critical strain rate for viscosity, the value of $\dot{\gamma}_{\mathrm{critical}}$ for pressure is higher because a higher shear rate is required to distort the radial distribution function than to distort the whole molecule. The trend of pressure changes due to strain rate observed here for hyperbranched polymer melts is similar to that seen previously in dendrimer melts and falls within the range between dendrimer and linear polymer melts.[19] This is because dendrimers have the most compact architecture, whereas hyperbranched polymers are less compact and linear polymers have the largest spatial separation of monomers. This behavior can be found not only for dendritic polymer melts but also for solutions. It has been reported by Lue[28] that dendritic polymers in low concentration solution have lower pressure than linear polymers. In addition, it was found that concentrated solutions of low-generation dendrimers show similar behavior to linear polymers and the pressure increases more rapidly with concentration for high-generation dendrimers.

B. Flow birefringence

In the presence of a velocity gradient, the statistical distribution of a flexible polymer is deformed from the equilibrium isotropic state and the refractive index of the solution becomes anisotropic. This phenomenon is called flow birefringence or the Maxwell effect. The birefringence of a polymer system due to the alignment of the intramolecular bonds is called intrinsic birefringence whereas that caused by the alignment of the whole molecules is called form birefringence.[25] The contribution to the birefringence effect from the alignment of molecules is more important in the case of solutions and arises due to the differences between the polarizability of the molecules and the solvent.

1. Form birefringence

In order to characterize the flow induced molecular alignment of hyperbranched polymers, the molecular order tensor $\mathbf{S}_m$ has been computed as

$$\mathbf{S}_m = \sum_{i=1}^{N} \left\langle \mathbf{u}_i\mathbf{u}_i - \frac{1}{3}\mathbf{I} \right\rangle,$$

where $\mathbf{u}_i$ is the unit vector denoting the orientation of the single molecules and N is the total number of molecules in

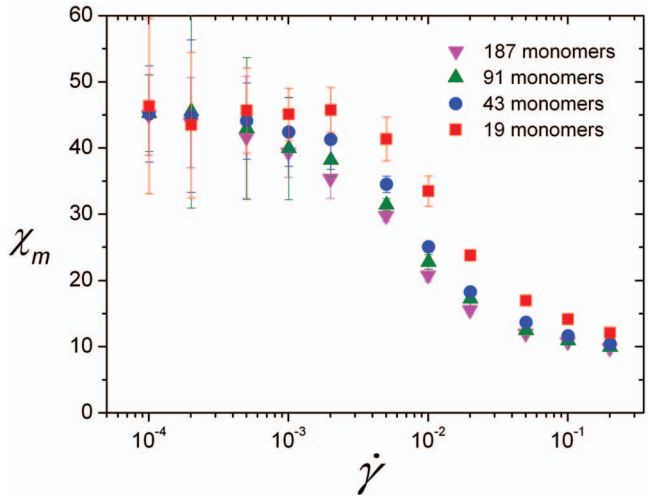

FIG. 9. Molecular alignment angle for hyperbranched polymers of different molecular sizes.

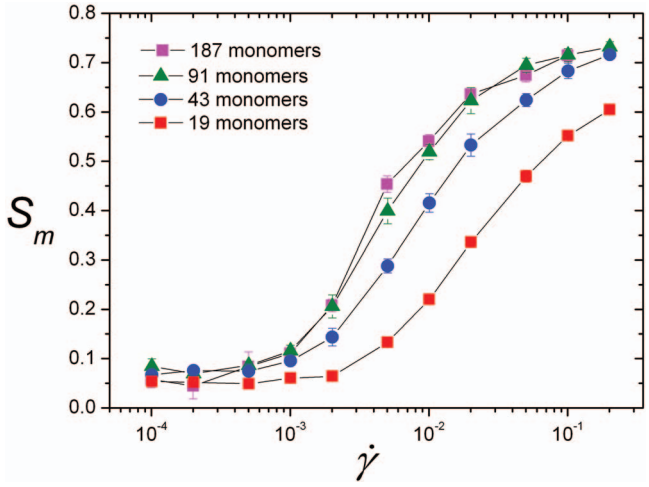

FIG. 10. Order parameter of the molecular alignment tensor for different hyperbranched polymers.

the system. The direction in which molecules are aligned is indicated by the eigenvectors of the order tensor. Assuming the eigenvector corresponding to the largest eigenvalue of the tensor of gyration denotes the orientation of the molecule $\mathbf{u}_i$, the birefringence extinction angle will be the angle between the flow direction and the molecular alignment direction.

Figure 9 shows the molecular alignment angle for different hyperbranched polymers. It can be seen that all simulated systems reach the Newtonian region with the alignment angle of 45° in the range of considered strain rates. The 45° angle is expected for systems in the Newtonian regime due to the nonuniform spin angular velocity of molecular rotation in shear flow. Furthermore the alignment angle of large hyperbranched polymers departs from 45° only at low strain rates whereas the alignment angle of small polymers remains close to 45° until higher strain rates are reached because these small polymers can rotate with the flow more easily. In comparison with other NEMD simulation data, our alignment angles in the non-Newtonian region are smaller than those for dendrimers and larger than those for linear polymers of the same molecular weight. This is because dendrimers have the most compact and constrained structure while hyperbranched polymers have less rigid architecture and linear polymers can stretch and align more easily with respect to the flow field, leading to anisotropic friction.

The order parameter S_m which describes the extent of the molecular alignment can be defined as 3/2 of the largest eigenvalue of the order tensor, which is a measure of the anisotropy of the average inertia tensor of a flexible molecule caused by the shear field.[25] This value equals zero in the case of orientational disorder and reaches one for perfect alignment. Figure 10 presents the molecular order parameter of different hyperbranched polymers. It remains constant at low strain rates and rapidly increases at high strain rate regions. This indicates that the orientational ordering increases and the alignment of the polymeric chains is more pronounced at high strain rates. It can also be seen that for any given strain rate larger N polymer systems have larger values of S_m in comparison to smaller N polymer systems. However when the number of beads increases, the gap between the values of S_m for hyperbranched polymers decreases. For the two largest systems of simulated hyperbranched polymers, the order parameter curves almost overlap. Furthermore, at the highest strain rate of 0.2, the order parameters for polymers comprising 43, 91, and 187 beads reach the same value of ~0.73.

2. Intrinsic birefringence

In order to characterize the intrinsic birefringence of hyperbranched polymer systems, the flow induced bond alignment has been analyzed. The bond alignment tensor can be calculated as

$$\mathbf{S}_{\text{bond}} = \sum_{i=1}^{N_s-1} \left\langle \mathbf{u}_i \mathbf{u}_i - \frac{1}{3}\mathbf{I} \right\rangle,$$

where N_s is the total number of beads in one molecule and $\mathbf{u}_i$ is the unit vector between neighboring beads which can be defined as

$$\mathbf{u}_i = \frac{\mathbf{r}_{i+1} - \mathbf{r}_i}{|\mathbf{r}_{i+1} - \mathbf{r}_i|}.$$

The flow alignment angle and the extent of the bond alignment can be calculated similarly to those of the molecular alignment in Sec. II B 1.

Figure 11 presents the bond alignment angle results for different hyperbranched polymers and linear polymers of equivalent molecular weight. As can be seen, the range of considered strain rates is wide enough for all hyperbranched polymer systems to reach the Newtonian regime where the bond alignment angle χ is 45°. In contrast, for large linear polymers of 91 and 187 beads per molecule, the bond alignment angle cannot reach 45° in the considered range of strain rate. In order to reach the alignment angle of 45°, the systems would have to be simulated at lower strain rates. It can also be seen that in the non-Newtonian region, the bond alignment angle decreases with increasing strain rate. At a given strain rate, the bond alignment angle of larger molecules is smaller than that of the smaller ones. Our data for

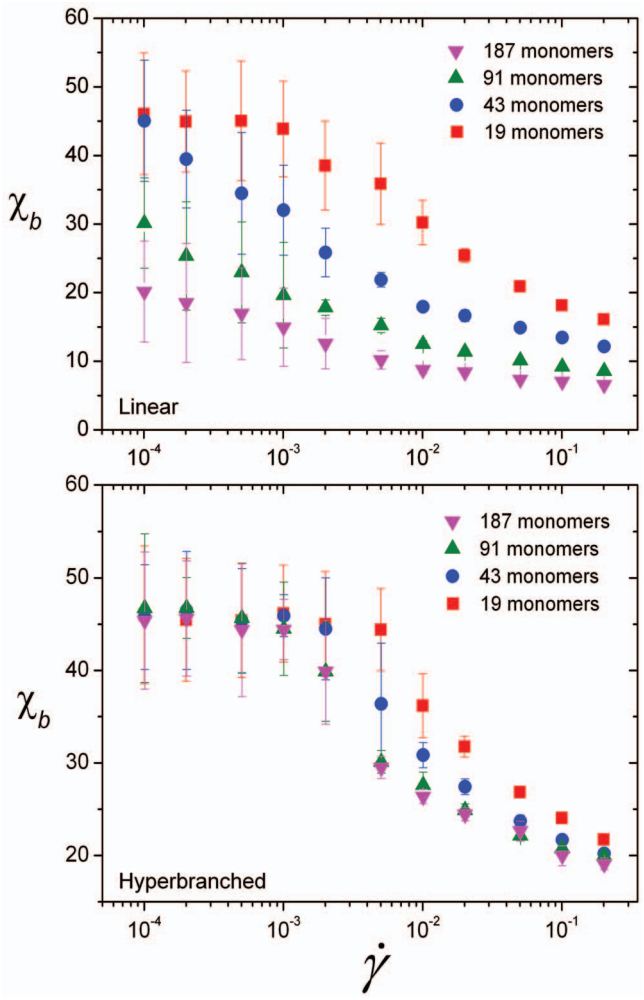

FIG. 11. Flow alignment angle for linear and hyperbranched polymers.

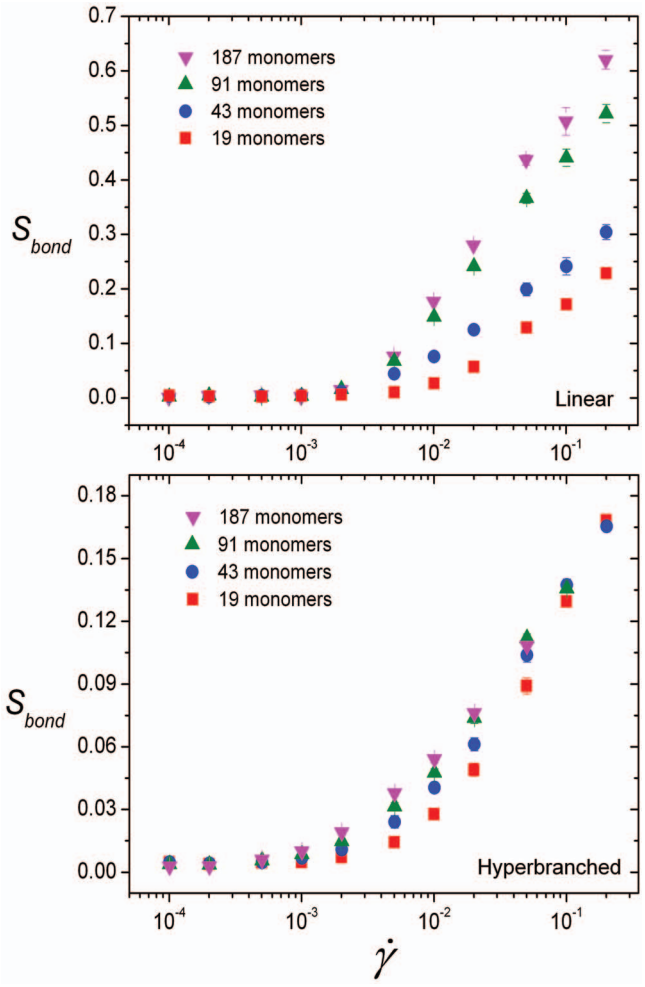

FIG. 12. Bond order parameter for linear and hyperbranched polymers.

linear polymers are in good agreement with other NEMD simulation results[29] which indicated that the bond alignment of systems comprising no more than 60 beads can reach the Newtonian regime in the range of strain rate we have investigated.

Alignment in the shear plane can be characterized by the values of S_{bond}, which are shown in Fig. 12. It can be clearly seen that for both hyperbranched and linear polymer systems, all these values increase with increasing strain rates, and at the same strain rate, values for larger polymers are always higher than those for smaller polymers. This implies that for a given strain rate, the chain segments in large molecules can more easily stretch and align with respect to the flow field. The S_{bond} function of shear rate is monotonically increasing, but at high strain rates the values of S_{bond} become the same for all hyperbranched polymer systems while those values are much higher for large linear polymers in comparison with small ones. Furthermore, at a given strain rate, the alignment parameter for hyperbranched polymers is always lower than that for linear polymers. This is because it is more difficult for hyperbranched chain segments to stretch and align with respect to the flow field as they have a more compact and constrained architecture. Our alignment results for linear polymers show good agreement with other NEMD simulation results[29] although our data show slightly stronger alignment due to the difference in temperature and chain length of the systems.

C. Stress optical rule

In order to characterize the relationship between macroscopic stress with the microscopic processes such as rotations and deformations of bonds,[30] the SOR can be tested from the bond alignment tensor and stress tensor. It states that the mechanical and optical tensors are coaxial and proportional to each other.

Figure 13 presents the ratio of $(P_{xx}-P_{yy})$ and $(S_{xx}-S_{yy})$, as well as that of $(P_{yy}-P_{zz})$ and $(S_{yy}-S_{zz})$, where P_{xx}, P_{yy} and P_{zz} are components of the pressure tensor and S_{xx}, S_{yy}, and S_{zz} are components of the bond alignment tensor, for hyperbranched polymers of different molecular weight. As can be seen, the components of the stress and alignment tensor are proportional at low strain rates. The proportionality constant, which is called the stress optical coefficient, is independent of molecular weight. For all hyperbranched polymer systems, this coefficient has the value of ~3.3(3). The independence of the stress optical coefficient on molecular weight for simulated hyperbranched polymers is in good agreement with experimental results which showed that the stress optical coefficient is a function of the local condition

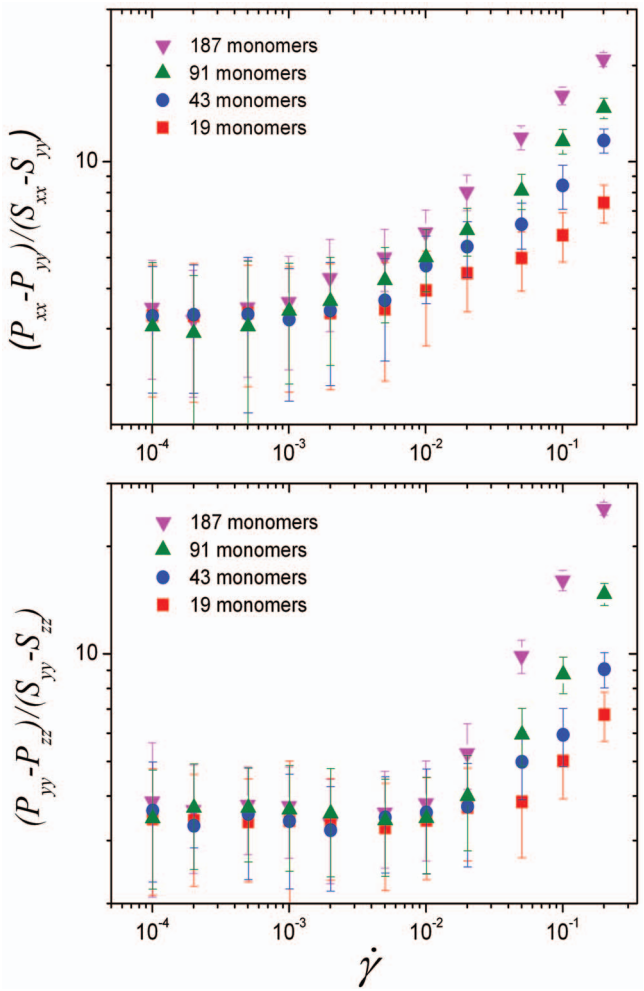

FIG. 13. Deviations from the stress optical rule-$(P_{xx}-P_{yy})/(S_{xx}-S_{yy})$ and $(P_{yy}-P_{zz})/(S_{yy}-S_{zz})$ vs the logarithm of $\dot{\gamma}$ for different hyperbranched polymers.

such as the temperature, solvent or polymer concentration but does not depend on the features of molecular structure on a large length scale such as molecular weight, molecular weight distribution, branching and degree of cross-linking.[25] At high strain rates, the SOR is invalid for all simulated hyperbranched polymers. The reason is that the microstructure of hyperbranched polymer melts is not included in the bond order tensor whereas the stress is determined by the alignment, deformation and microstructure of the systems. The SOR does not take into account the flow-induced changes of the radial distribution function which is distorted at high strain rates.

It has been discussed elsewhere that the failure of the SOR could be due to the influence of the molecular weight distribution,[31] the chain conformation,[32] or the role of the number of entanglements in the fluid.[33] There are also certain types of systems that do not follow the SOR at all such as rodlike polymers in the concentrated isotropic regime.[34] In experiments, the experimental conditions can also lead to the failure of the SOR, such as performing experiments near the glass transition temperature[30,35] or at a rate higher than the inverse of the Rouse time of the chain in an elongational experiment.[36] The SOR fails also because while birefringence saturates, the stress can continue to grow without limit.[37] These factors are not present in our study, hence we can deduce that the SOR is violated as flow-induced changes of the microstructure of hyperbranched polymers were not taken into account.

III. CONCLUSIONS

In this work, NEMD simulations have been performed for four different hyperbranched polymer structures with molecular weight varying from 19 to 187. Rheological properties of these polymer melts were characterized and the crossover from Newtonian to non-Newtonian behavior was captured in the considered range of strain rates. Computed shear viscosities are slightly higher than those for dendrimers and much lower than those for linear polymers of equivalent molecular weight, which is in accordance with the molecular architecture being more open than that of dendrimers and much more compact than that of linear analogs. Shear thinning is observed for all hyperbranched polymer fluids although it occurs at different strain rates for different systems. Normal stress coefficients were also calculated and were shown to have very large power-law regions. The magnitude of the second normal stress coefficient is ~20% of the first normal stress coefficients. In all cases, the obtained pressure of the polymeric fluid remains approximately constant at low strain rates and rapidly increases at very high strain rates.

The flow birefringence of hyperbranched polymer melts has also been characterized by taking into account the calculation of the form and intrinsic birefringence. For all systems, the flow alignment angle converges to 45° at low strain rates and the order parameter results have shown that the intrinsic birefringence is fairly small in comparison with the form birefringence. Furthermore, the SOR has been shown to be valid only in the Newtonian regime. The stress optical coefficient of ~3.3(3) does not depend on the molecular weight of hyperbranched polymers. In our systems, the SOR fails in the non-Newtonian region because it does not take into account the flow-induced changes of the microstructure.

ACKNOWLEDGMENTS

We would like to thank Swinburne University of Technology Supercomputer Facility for a generous grant of computer time. One of the authors (T.C.L.) would like to thank Dr. Jaroslaw Bosko for his valuable suggestions and discussions.

[1] C. Gao and D. Yan, Prog. Polym. Sci. **29**, 183 (2004).
[2] T. C. Le, B. D. Todd, P. J. Daivis, and A. Uhlherr, J. Chem. Phys. **130**, 074901 (2009).
[3] Y. H. Kim and O. W. Webster, Macromolecules **25**, 5561 (1992); Y. H. Kim and R. Beckerbauer, *ibid.* **27**, 1968 (1994).
[4] I. Bodnar, A. S. Silva, R. W. Deitcher, N. E. Weisman, Y. H. Kim, and N. J. Wagner, J. Polym. Sci. Part Polym. Phys. **38**, 857 (2000); I. Bodnar, A. S. Silva, Y. H. Kim, and N. J. Wagner, *ibid.* **38**, 874 (2000).
[5] C. R. Yates and W. Hayes, Eur. Polym. J. **40**, 1257 (2004).
[6] R. B. Bird, C. F. Curtiss, R. C. Armstrong, and O. Hassager, *Dynamics of Polymeric Liquids* (Wiley, New York, 1987).
[7] P. J. Farrington, C. J. Hawker, J. M. J. Frechet, and M. E. Mackay, Macromolecules **31**, 5043 (1998).
[8] T. T. Hsieh, C. Tiu, and G. P. Simon, Polymer **42**, 7635 (2001); **42**, 1931 (2001).

[9] S. B. Kharchenko, R. M. Kannan, J. J. Cernohous, S. Venkataramani, and G. N. Babu, J. Polym. Sci. Part Polym. Phys. **39**, 2562 (2001).
[10] S. Kunamaneni, D. M. A. Buzza, D. Parker, and W. J. Feast, J. Mater. Chem. **13**, 2749 (2003); Suneel, D. M. A. Buzza, D. J. Groves, T. C. B. McLeish, D. Parker, A. J. Keeney, and W. J. Feast, Macromolecules **35**, 9605 (2002).
[11] S. P. Gretton-Watson, E. Alpay, J. H. G. Steinke, and J. S. Higgins, Ind. Eng. Chem. Res. **44**, 8682 (2005).
[12] J. D. Weeks, D. Chandler, and H. C. Anderson, J. Chem. Phys. **54**, 5237 (1971).
[13] G. S. Grest and K. Kremer, Phys. Rev. A **33**, 3628 (1986).
[14] D. J. Evans and G. P. Morriss, *Statistical Mechanics of Nonequilibrium Liquids* (Academic, London, 1990).
[15] C. W. Gear, *Numerical Initial Value Problems in Ordinary Differential Equations* (Prentice-Hall, Englewood Cliffs, 1971).
[16] B. D. Todd and P. J. Daivis, Mol. Simul. **33**, 189 (2007).
[17] M. M. Cross, J. Colloid Sci. **20**, 417 (1965).
[18] K. Yasuda, J. Textile Engineering **52**, 171 (2006).
[19] J. T. Bosko, B. D. Todd, and R. J. Sadus, J. Chem. Phys. **121**, 12050 (2004).
[20] I. Sendijarevic and A. J. McHugh, Macromolecules **33**, 590 (2000).
[21] C. J. Hawker, P. J. Farrington, M. E. Mackay, K. L. Wooley, and J. M. J. Frechet, J. Am. Chem. Soc. **117**, 4409 (1995); S. Uppuluri, F. A. Morrison, and P. R. Dvornic, Macromolecules **33**, 2551 (2000).
[22] T. Kairn, P. J. Daivis, M. L. Matin, and I. K. Snook, Polymer **45**, 2453 (2004).
[23] L. I. Kioupis and E. J. Maginn, Chem. Eng. J. **74**, 129 (1999).
[24] J. T. Bosko, Swinburne University of Technology, 2005.
[25] M. Doi and S. F. Edwards, *The Theory of Polymer Dynamics* (Clarendon, Oxford, 1986).
[26] A. Jabbarzadeh, J. D. Atkinson, and R. I. Tanner, Macromolecules **36**, 5020 (2003); P. J. Daivis, M. L. Matin, and B. D. Todd, J. Non-Newtonian Fluid Mech. **147**, 35 (2007).
[27] J. D. Ferry, *Viscoelastic Properties of Linear Polymers* (Wiley, New York, 1980).
[28] L. Lue, Macromolecules **33**, 2266 (2000).
[29] M. Kroger, W. Loose, and S. Hess, J. Rheol. **37**, 1057 (1993).
[30] J. L. S. Wales, *The Application of Flow Birefringence to Rheological Studies of Polymer Melts* (Delft University Press, Delft, 1976).
[31] J. van Meerveld, J. Non-Newtonian Fluid Mech. **123**, 259 (2004).
[32] T. Sridhar, D. A. Nguyen, and G. G. Fuller, J. Non-Newtonian Fluid Mech. **90**, 299 (2000).
[33] J. P. Rothstein and G. H. McKinley, J. Non-Newtonian Fluid Mech. **108**, 275 (2002).
[34] D. W. Mead and R. G. Larson, Macromolecules **23**, 2524 (1990).
[35] M. Kroger, C. Luap, and R. Muller, Macromolecules **30**, 526 (1997).
[36] D. C. Venerus, S. H. Zhu, and H. C. Ottinger, J. Rheol. **43**, 795 (1999).
[37] M. H. Wagner, Korea-Aust. Rheol. J. **18**, 199 (2006).